Inhomogeneity and the metal-insulator transition for disordered systems

T. G. Castner
Department of Physics and Applied Physics, University of Massachusetts Lowell, Lowell, Massachusetts 01854, USA
(Received 19 February 2003; published 2 September 2003)

The effect of both macroscopic stress inhomogeneity and doping inhomogeneity on the critical behavior of the conductivity in the vicinity of the metal-insulator transition are calculated. For the uniaxial stress case the inhomogeneity is calculated from the bending deflection $d(z)$ of a column under compression. It is the transverse variation in doping or stress S that can produce a substantial increase in the scaling exponent t of the $T\rightarrow 0$ conductivity and change the critical stress S_c to an apparent critical stress S_c^*. It is demonstrated the calculated results can explain the experimental results of uniaxial stress experiments for Si:P and Si:B. In these cases when $\sigma(S,T\rightarrow 0)$ is sufficiently large $\sigma(S,T=0)\propto|S/S_c-1|^t$ with $t\sim\frac{1}{2}$, but when $\sigma(S,T=0)$ is sufficiently small $\sigma(S,T=0)\propto|S/S_c^*-1|^{t_{\rm eff}}$ with $t_{\rm eff}$ between 1 and 1.6 dependent on geometrical factors. For the doping inhomogeneity case both uncorrelated dopant density variations and correlated linear dopant variations are considered. Correlated cases can either increase or decrease n_c depending on the geometry of the doping gradients. An uncorrelated broad distribution can mask scaling behavior with an exponent $t=\frac{1}{2}$ and change the exponent to $t\sim 1$. This suggests that the microscopic physics may be the same for crystalline doped semiconductors Si:P, Ge:Ga, and the amorphous semiconductor-metal cases and that the difference in scaling exponents of the conductivity results from the breadth and shape of the distribution $P(n(\mathbf{r})-n)$. A large width of $P(n(\mathbf{r})-n)$ for a-$S_{1-x}M_x$ alloys helps explain why the conductivity prefactors are comparable to Si:P; etc., even though the electron density is 10^3 larger.

DOI: 10.1103/PhysRevB.68.115201 PACS number(s): 71.30.+h, 72.15.−v, 72.20.Fr, 72.80.Ng

I. INTRODUCTION

The metal-insulator transition (MIT) in doped semiconductors [Si:P, Ge:Ga, etc.] and in amorphous (a) semiconductor-metal alloys [a-$Si_{1-x}Nb_x$, a-$Ge_{1-x}Au_x$, etc.] has been studied for decades. In the last two decades much attention has focused on the critical behavior of the conductivity in the limit of zero temperature as the critical point is approached. Several approaches have been employed to "tune" the MIT and to approach the critical point. The standard approach has been to study samples with different concentrations of donors for Si:P or the variation of $x-x_c$ for the a-S-M alloys. The difficulty with this approach is that very close to the critical point [n_c for Si:P, x_c for a-$Si_{1-x}Nb_x$] small variations in the doping or composition across the sample can affect the critical behavior and scaling exponent. An attractive alternative approach to tune through the critical point and obtain critical exponents has been through the tuning of an external parameter such as uniaxial stress[1–3] or a magnetic field. The magnetic field case involves a change of universality class[4] to unitary and the increase in the scaling exponent toward 1 has been observed for Si:B (Ref. 5) and Si:P (Ref. 6). For the magnetic field case the field inhomogeneity is very small and will not be discussed herein. However, the uniaxial stress case under a compressive stress S also is confronted by an intrinsically serious problem in the vicinity of a critical point where the stress dependent conductivity $\sigma(S,T\rightarrow 0)\rightarrow 0$ as $S\rightarrow S_c$—namely, the introduction of stress inhomogeneity (SI) caused by a small sample bending deflection. It should be emphasized that there are numerous uniaxial stress experimental results where the effect of SI is small and not sufficiently important to affect the interpretation of the physics. The uniaxial stress results of Wilson and Feher[7] determining the g-tensor values g_ℓ and g_t for the SI conduction-band valleys represent one such case, while the stress-induced splittings of the donor-excited states by Aggarwal and Ramdas[8] are another example. In the critical regime SI can play a dominant role and substantially alter the scaling exponent, in addition to introducing an apparent critical stress S_c^* different than S_c. An important issue still actively debated is the breadth of the critical regime (CR). The breadth of the CR and the possible crossover from one critical exponent to another will be affected by doping inhomogeneity (DI) or SI. Inhomogeneity and its effect on the scaling exponent of $\sigma(n,S,T\rightarrow 0)=\sigma_0(n/n_c-1)^t$ in the vicinity of the critical point is the subject of this paper.

The subject of the piezoresistance of semiconductors is nearly as old as the study of semiconductors themselves. Following the discovery of the piezoresistance effect in doped Ge and Si by Smith,[9] there were a series of studies[10–14] of the piezoresistance of doped Ge and Si in the next decade. The early strain-induced effects in semiconductors have been reviewed by Bir and Pikus.[15] The most relevant of these studies to the present subject are the results on degenerate Ge:Sb and Ge:As by Cuevas and Fritzsche.[14] These authors were concerned with the possible effect of SI for their transverse piezoresistance experiment because of large friction and the possible bulging of their rectangular bar. Despite the concerns of these experimental groups with SI from sample buckling in compression the data gave no evidence of SI from sample bending. The basic reason for this is that these early studies were not sufficiently close to the critical point at n_c (S_c) at $T=0$. These early piezoresistance studies were at $T\geqslant 1.2$ K and $\sigma(n,S,T)$ was not small enough for the SI effect from sample bending to be easily measurable.

Controversy over the role of inhomgeneity in the MIT

field arose nearly three decades ago. Cohen and Jortner[16] proposed an inhomogeneous regime near the critical point composed of metallic and insulating regions. They viewed the MIT as the approach to a percolation threshold and that the conductivity could be treated by effective medium theory. Their approach as $x \rightarrow x_c$ from the metallic side is characterized by conducting ''channels'' that get smaller as the insulating islands grow. Mott,[17] who formulated the idea of a minimum metallic conductivity, used theoretical arguments to argue that one could not have large insulating regions in a barely metallic sample. At this time the data to definitively rule out Mott's $\sigma_{\min \text{ met}}$ were not yet available. At the same time there was extensive work on percolation theory which has been reviewed by Kirkpatrick.[18] The much older effective medium theory (EMT) has been applied to applied to electrical transport of mixtures such as the alkali-tungsten bronzes[19] (Na_xWO_3). These studies demonstrated that EMT broke down for $C<0.4$ when the conductivity ratio $r=\sigma_I/\sigma_M$ (<0.01) is small and the percolation threshold C^* is considerably less than the site percolation threshold p_c. Scher and Zallen[20] proposed $C^*=fp_c$, where f is the packing fraction leading to $C^* \approx 0.15$ for the continuous percolation problem. Skal *et al.*[21] obtained $C^*=0.17$ from numerical studies for a particular random potential with site correlations up to third nearest neighbors. For $I_{1-x}M_x$ systems with $r \ll 0.01$ the notion was that $\sigma(C)$ should obey the Kirkpatrick percolation prediction $\sigma(C) \propto (C-C^*)^{1.6}$ for $C<0.5$. It is to be noted that the a-$S_{1-x}M_x$ systems do show values x_c ($x_c=C^*$) somewhat less than $C^*=0.15$, but do not exhibit the percolation exponent of 1.6. For Na_xWO_3 Lightsey[22] reported $x_c=0.16\pm0.03$ and $t=1.8\pm0.2$ in agreement with the percolation prediction.

This was followed by the scaling approach to the MIT Wegner[23] showed the $T=0$ conductivity to be of the form $\sigma \propto (E_F-E_c)^{(d-2)\nu}$ where E_F is the Fermi energy, E_c the mobility edge dividing localized and itinerant states, d the dimensionality of the system, and ν the correlation length exponent. Several years later, Abrahams *et al.*[24] employed the $\beta(g)$-function approach to obtain a scaling result similar to that of Wegner. These results for $d=3$ and $\nu \sim 1$ appeared to explain experimental results[25–28] that followed in the 1980s on the a-S-M alloys. However, comprehensive low-temperature studies[29] of Si:P established that $\sigma(n,T \rightarrow 0)$ scaled toward zero with an exponent $t \sim \frac{1}{2}$. These studies were the first to clearly demonstrate values of $\sigma(n,T \rightarrow 0)$ substantially less than Mott's prediction [$\sigma_{\min \text{ met}} \sim 20$ S/cm for Si:P]. These experiments were followed by the pioneering studies of Paalanen, Rosenbaum, Thomas, and Bhatt[2] (PRTB) on the uniaxial compression experiments that verified the $t \sim \frac{1}{2}$ scaling exponent. These authors made no effort to analyze the tail region of $\sigma(S,T \rightarrow 0)$ that occurred for $\sigma<5$ S/cm. However, the recent experiment results of Bogdanovich, Sarachik, and Bhatt[2] (BSB) and Waffenschmidt, Pfleiderer, and v. Löhneysen[3] (WPL) both yield a larger exponent ($t \sim 1.6$ for BSB and $t \sim 1.0$ for WPL), but the analysis was of the tail region. WPL claim the critical regime is for $\sigma<\sigma_{cr} \approx 12$ S/cm; however, this is precisely the tail region where the transport is affected by large SI. Neither BSB nor WPL emphasize that their results for larger values of σ yield an exponent t near $\frac{1}{2}$ in good agreement with the pioneering results[1] of PRTB. This paper demonstrates that the crossover to a larger exponent in the tail regime for small values of $\sigma(S,T \rightarrow 0)$ is explained by SI. A brief account[30] of the effect of SI from simple sample bending has been given that explains the BSB exponent of 1.6.

The SI results have demonstrated that correlated SI in compression experiments can dramatically alter the scaling exponent for small values of $\sigma(S,T \rightarrow 0)$. This suggests further studies of the role of DI are warranted. These studies suggest a different explanation for the scaling exponent $t \sim 1.0$ observed for the a-$S_{1-x}M_x$ systems based on a broad distribution $P(n-\underline{n})$. This in turn suggests the possibility there may be a common origin of the microscopic behavior of the conductivity of systems like Si:P, Ge:Ga, etc., and the a-$S_{1-x}M_x$ alloys.

II. STRESS INHOMOGENEITY

The uniaxial stress experiments demonstrate an approximate linear dependence between S and n and S tunes the critical density n_c. This is represented by the relation $S-S_c=k(n-n_c)$, where k is a constant determined from experiment. The theoretical situation for Si:P has been treated in detail by Bhatt,[31] who calculates the change in n_c with S. For Si:P stress admixes some of the $1s$-E state into the ground $1s$-A_1 state and effectively increases the Bohr radius a^* of the ground state band and, through the Mott criterion, decreases n_c. Thus uniaxial stress S makes Si:P more metallic. The experiments start with an insulating sample, which becomes metallic when S exceeds S_c. The mechanism for Si:B involves the degeneracy of the valence band in the vicinity of $\mathbf{k}=0$ and has the opposite sign of that for Si:P and an order of magnitude smaller proportionality constant k between S and p (hole concentration). The treatment of SI on the scaling behavior on $\sigma(S,T \rightarrow 0)$ given below does not depend on the details of S versus n or p. The factor S/S_c-1 used for Si:P is replaced by $1-S/S_c$ for Si:B.

A particularly straight forward case of SI results from sample bending that occurs in uniaxial stress experiments with compression loading. Under compression, columns undergo a small deflection. The solution of the column equation $EId^2y/dz^2=-M(y)=-Py$ yields a solution $y(z)=d_m \sin(\pi z/L)$ for free or pinned ends where L is the length of the column, E is Young's modulus, I is the column cross-section [area $A=ab$, $a<b$, bending is about an axis perpendicular to a] moment of inertia, $M(y)$ is the bending moment produced by the axial load P, and the deflection y. The deflection of the column will be designated $d(z)=d_m \sin(\pi z/L)$. The maximum deflection depends on the slenderness ratio $(L/a)^2$, the eccentricity of the axial loads P at each end of the column, and the quality and rigidity of the load bearing surfaces applying the load P. The bending leads to a stress distribution $S(y,z)$ of the form

$$S(y,z)=P/A[1+12yd(z)/a^2], \quad -a/2<y<a/2. \quad (1)$$

This distribution differs from the correlated DI case discussed below because the y and z dependences are coupled.

The bending will ordinarily be about an axis with the smallest moment of inertia (in this case $I_a = ba^3/12$), although when the cross section is nearly square, the bending may be more complex. The two-dimensional stress distribution is an excellent approximation since $a < \frac{1}{2}b$ applicable to the PRTB and BSB experimental results; however, for the WPL experiment, $a = 0.8$ mm and $b = 0.9$ mm and the nearly square cross section could lead to a three-dimensional stress distribution. In addition, we ignore any shear stress effects from torsion. Torsion effects could only occur if the axial load P applied at each end of the column also applied a torque about the column axis (z axis). Equation (1) shows the stress varies from $\underline{S}(1-6d(z)/a)$ to $\underline{S}(1+6d(z)/a)$ where $\underline{S} = P/A$. A rather small deflection of 0.01 mm (about 0.1% of the length L) leads to a 40% variation in $S(y,z)$ across the cross section of the column. This leads to a normalized stress distribution $f(S)$ $[\int f(S)dS = 1]$ of the form

$$f(S) = 1/2\underline{S}\lambda(z), \quad \underline{S}(1-\lambda) < S < \underline{S}(1+\lambda),$$

$$\lambda(z) = 6d(z)/a, \tag{2}$$

and $f(S) = 0$ outside this range. It is straightforward to show that the average stress across a cross section at z is $\underline{S}$ independent of z because the second term in Eq. (1) makes no contribution to the integral $a^{-1}\int_{-a/2}^{a/2} S(y,z)dy = \underline{S}$. This is a requirement for static equilibrium of the column.

Ignoring SI and considering a homogeneous stress distribution the $T = 0$ conductivity has been shown to be of the form $\sigma(S) = \sigma_0|S/S_c - 1|^t$ in the PRTB, BSB, and WPL experiments. An integration over a cross section at an arbitrary z yields the result $\sigma(z) = \sigma_0 \int (S/S_c - 1)^t f(S)dS$. With Eq. (1) this can be converted to an integral over y. For large enough values of $\sigma(z)$ with all values of $S(y,z) > S_c$ one obtains the result

$$\sigma(z) = \sigma_0[S_c/2\underline{S}\lambda(z)(t+1)]\{[\underline{S}/S_c - 1 + \lambda(z)\underline{S}/S_c]^{t+1} - [\underline{S}/S_c - 1 - \lambda(z)\underline{S}/S_c]^{t+1}\}. \tag{3}$$

For the regime $\underline{S}/S_c - 1 \gg \lambda\underline{S}/S_c$ a series expansion of Eq. (3) leads to the result

$$\sigma(z) = \sigma_0(\underline{S}/S_c - 1)^t[1 + O(\lambda\underline{S}/S_c/(\underline{S}/S_c - 1))^2 + \cdots]. \tag{4}$$

The SI is unimportant in this regime, and the scaling behavior is the same as if there were no SI. For the limit of $\sigma(z)/\sigma_0 \ll 1$ and $\underline{S}/S_c - 1 \ll \lambda\underline{S}/S_c$ one needs to alter the lower limit of the integral. Since, for $S < S_c$, $\sigma(S) = 0$, the lower limit y^* is determined by the condition $S_c = \underline{S}(1 + 12d(z)y^*/a^2)$. Using $dS = \underline{S}(12d(z)dy/a^2)$ and $f(S)ds = dy/a$, the integral for $\sigma(z)$ becomes

$$\sigma(z) = (\sigma_0/a)\int_{y^*}^{a/2} \{\underline{S}/S_c - 1 + [12d(z)y/a^2]\underline{S}/S_c\}^t dy. \tag{5}$$

Only the upper limit contributes since the integrand is zero for the lower limit. The final result is

$$\sigma(z) = \sigma_0 a[(S_c/\underline{S})/12d(z)][\underline{S}/S_c - 1 + (6d(z)/a)\underline{S}/S_c]^{t+1}. \tag{6}$$

Although the integration over z between the voltage electrodes is yet to be done, it is worth discussing the result in Eq. (6). For $\underline{S} = S_c$, corresponding to $y^* = 0$ with half the cross section insulating ($y < 0$) and half the sample metallic ($y > 0$), $\sigma(z)$ becomes $(\sigma_0/2)(6d(z)/a)^{1/2}$. Here $6d(z)/a$ is a direct measure of the SI due to bending of the sample. Since S_c is the true critical stress in the absence of sample bending, an independent determination of S_c and $\sigma(S_c, T \to 0)$ provides a direct measure of the deflection $d(z)$ and SI, and $\sigma(z) = 0$ for $\underline{S}/S_c = 1/[1 + 6d(z)/a]$. This is the logical definition of the apparent critical stress $S_c^*(z)$. The two results of the linear stress variation across the cross section are (1) a lowering of the critical stress from S_c to S_c^* and (2) the crossover from a scaling exponent t without SI to a scaling exponent $t+1$ in the presence of SI. Here $S_c^*(z)$ *depends on the deflection* $d(z)$; *however, the scaling exponent* $t+1$ *is independent of* z. However, the actual critical behavior of $\sigma(\underline{S}, T \to 0)$ in the vicinity of S_c^* is more complex and depends on the details of the integration over z.

A comparison with the experimental data requires an integration over z between the voltage electrodes at z_1 and z_2 ($z_2 - z_1 = 1.0$ mm for the BSB Si:B sample, but is 6.0 mm for the WPL sample). The electrodes are not necessarily symmetrical about the maximum value of $d(z) = d_m$. In typical transport experiments with a constant-current source one measures the resistance R between the two electrodes, which leads to $R = (1/A)\int_{z1}^{z2}\rho(z)dz = (1/A)\int_{z1}^{z2} dz/\sigma(z)$. This leads to a value $\langle\sigma\rangle_{\text{expt}}$ obtained in the experiment is given by $\langle\sigma\rangle_{\text{expt}} = (z_2 - z_1)/\int_{z1}^{z1} dz/\sigma(z)$. One finds

$$\langle\sigma(w)\rangle_{\text{expt}} = [\sigma_0/2(t+1)w] \times (z_2 - z_1) \Big/ \int_{z1}^{z2} \lambda(z)/[w - 1 + \lambda(z)w]^{t+1} dz, \tag{7}$$

where $w = \underline{S}/S_c$ and $\lambda(z) = 6(d_m/a)\sin(\pi z/L)$. This integral, although apparently simple, does not lead to a simple analytical result for $t = \frac{1}{2}$ except for $w = 1$. It is readily and accurately evaluated numerically as a function of the parameter w (for the BSB case $w - 1$ is replaced by $1 - w$). The behavior of $\rho(z) = 1/\sigma(z)$ versus z is shown in Fig. 1 for four values of $\underline{S}/S_c$ approaching the apparent critical stress S_c^* appropriate to the WPL results for Si:P. Far from S_c^* ($\underline{S}/S_c = 1.2$), $\rho(z)$ is relatively flat and $\langle\sigma\rangle_{\text{expt}}$ is closely given by $\sigma(z)$. However, as $\underline{S} \to S_c^*$, $\rho(z)$ becomes increasingly sharply peaked at the "pinchoff" point at z_1. An increasingly large fraction of the voltage drop is associated with the peak, and $\langle\sigma\rangle_{\text{expt}}$ is no longer given even approximately by the average of $\sigma(z)$ between z_1 and z_2. In the limit $\underline{S} \to S_c^*$ the integral is dominated by the contribution from the z region near the peak and is qualitatively different from the flat case. Here $\rho_{\text{peak}} \propto (\underline{S}/S_c^* - 1)^{-(t+1)}$ and the width of the peak is $w_{\text{peak}} \propto (\underline{S}/S_c^* - 1)$ (demonstrated from the integration) and in this regime $\langle\sigma\rangle_{\text{expt}} \propto (z_2 - z_1)/\rho_{\text{peak}} w_{\text{peak}} \propto (\underline{S}/S_c^* - 1)^t$. In

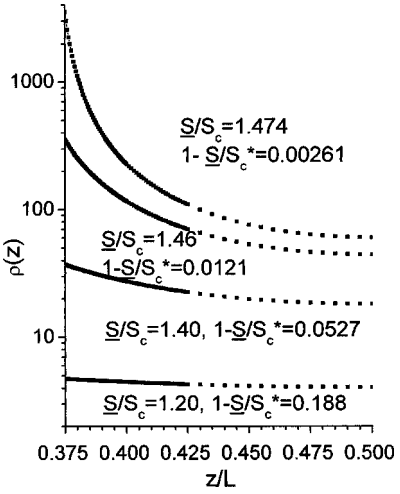

FIG. 1. Variation of $\rho(z)$ vs z between the two voltage electrodes as $z_1/L=0.375$ and $z_2/L=0.500$ for four different values of $1-\underline{S}/S_c^*$ approaching the apparent critical stress S_c^*. Far from S_c^*, $\rho(z)$ is relatively flat with only a small increase as z approaches z_1. As $\underline{S}$ more closely approaches S_c^*, $\rho(z)$ becomes more sharply peaked as $z\rightarrow z_1$. Approaching the pinchoff at $\underline{S}=S_c^*$, the integral $\int\rho(z)dz$ is dominated by the peak and the effective scaling exponent reverts to the original value of $t=\frac{1}{2}$.

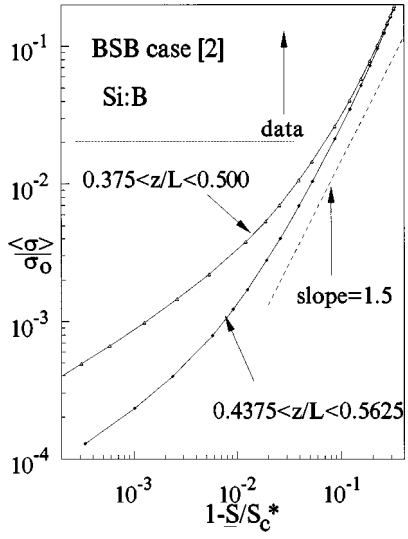

FIG. 2. Extension of $\langle\sigma\rangle/\sigma_0$ vs $1-\underline{S}/S_c^*$ based on the BSB parameters to much smaller values of $1-\underline{S}/S_c^*$ calculated with Eq. (7). For $1-\underline{S}/S_c^*<3\times10^{-3}$ the slope approaches the original exponent $t=\frac{1}{2}$.

this extreme limit (not yet reached by experimentalists) the scaling exponent t would be the same as in the case for large values of $\sigma(\underline{S},T=0)$ where SI is small. The integral in Eq. (7) has been evaluated for parameters appropriate for the BSB and WPL experimental results.

The BSB Si:B data for compressive uniaxial stress represent a nearly ideal case of SI from bending of a slender column. The voltage electrode spacing $z_2-z_1=L/8$ is small enough that the quantity $\lambda(z)$ [see Eq. (2)] does not vary much and the ratio of the apparent critical stress S_c^* to the true critical stress S_c is given reliably by $S_c^*/S_c\sim[1-\langle\lambda(z)\rangle]^{-1}$. BSB reported $S_c^*=613$ bars and a scaling exponent of 1.6 [using $\sigma(\underline{S},T\rightarrow0)=\sigma_0(1-\underline{S}/S_c^*)^t$]. My prior analysis[30] demonstrated $S_c^*/S_c\sim1.53$ corresponding to $\langle\lambda(z)\rangle\sim0.346$ and $S_c=400\pm15$ bars. The BSB data for $\sigma(\underline{S},T\rightarrow0)>20$ S/cm yield $t=0.51$ for $S_c=400$ bars and $\sigma_0\approx52.34$ S/cm. Employing Eq. (7) for $w=1$, one finds $\langle\sigma(\underline{S}=S_c,T=0)\approx10.3$ S/cm which is 0.86 of the experimental value 12 S/cm for $\underline{S}=400$ bars. The experimental uncertainty in $S_c\sim400$ bars is $\pm4\%$. There is some uncertainty in the analysis dependent on the parameters. If the voltage electrodes are asymmetrical with respect to the point of maximum deflection $[\lambda(z)=\lambda_m]$, then the parameters change a small amount.

The quantity $\langle\sigma\rangle/\sigma_0$ from Eq. (7) is shown versus $\underline{S}/S_c^*-1$ in Fig. 2 for two positions of the voltage electrodes. The symmetric case $(0.4375<z/L<0.5625)$ show a slope slightly larger than $t+1=1.5$ for $\underline{S}/S_c^*-1>0.03$. At smaller values of $\underline{S}/S_c^*-1$ there is a crossover to a slower dependence, and for $\underline{S}/S_c^*-1<0.001$ there is a new exponent $t\sim0.5$: namely, the same scaling exponent as seen in seen in the BSB data for values of $\langle\sigma(\underline{S})\rangle>20$ S/cm. However, the experimental data in BSB for metallic samples [$\underline{S}<613$ bars] are limited to $\sigma>2$ S/cm. This is shown by the horizontal dashed line in Fig. 2. The BSB data extended to 59 mK. If the data were extended to the 3 mK reached by PRTB, the $\sqrt{T}$ dependence would reduce $\sigma(\underline{S}=613\text{ bars},T)$ by a factor of 4.4 and would permit a more accurate determination of the actual cutoff at S_c^*. Although BSB obtained a good fit to finite-T scaling with $S_c^*=613$ bars, a more accurate determination of S_c^* would require data to much lower T. One notes that the calculated value $\langle\sigma\rangle/\sigma_0$ falls off more slowly for the asymmetric case $[0.375<z/L<0.500]$ and deviates from the slope $t+1=1.5$ for much smaller values of $1-\underline{S}/S_c^*$. The asymmetric case approaches the $t\sim0.5$ result from the ''pinchoff'' faster than the symmetric case and is already in this regime for $\underline{S}/S_c^*-1\sim0.003$. For the experimental data for Si:B to approach this closely to S_c^* would require a stress resolution of less than about 2 bars or about one order of magnitude better resolution in $\underline{S}$ than obtained by BSB. Nevertheless, the calculated results in Fig. 2 for $\langle\sigma\rangle/\sigma_0>0.02$ are in excellent agreement with the BSB result of $t+1\sim1.6$. The deflection required to explain the linear SI in the BSB results is $d_m=\langle\lambda\rangle a/6=0.017$ mm [$a=0.3$ mm for the BSB sample], which is 0.2% of the length L of the sample. BBS (Ref. 32) in their response to Ref. 30 have argued it is unlikely that one would get this large a deflection for their loads $\underline{S}$ because they are a small fraction of the Euler critical stress $S_c=\pi^2EI/L^2$. This issue will be considered in more detail in the Discussion.

The data from WPL for $\sigma(\underline{S},T\rightarrow0)$ versus $\underline{S}$ are given in Fig. 3. The five largest values of σ are a reasonable fit to scaling of the form $\sigma=\sigma_0(\underline{S}/S_c-1)^t$ for $\sigma>6$ S/cm. An optimized (minimum standard deviation) numerical fit to these five points yields $t=0.59$, $S_c=1.915$ kbar, and $\sigma_0=20.3$ S/cm. The dashed line is the extension of this fit to $\sigma=0$ and $\underline{S}=S_c$. A slightly poorer fit with $S_c=1.99$ can yield $t=\frac{1}{2}$. The WPL data for $\sigma(\underline{S},T\rightarrow0)<6$ S/cm yield an

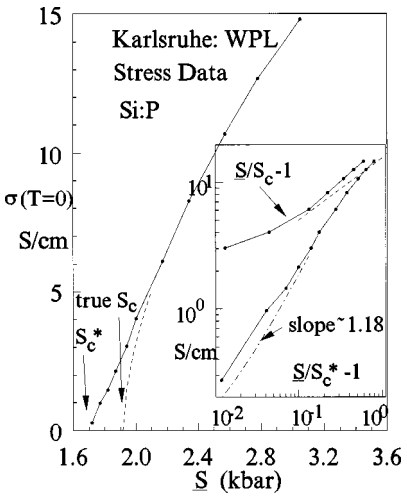

FIG. 3. WPL $\sigma(\underline{S},T\rightarrow 0)$ vs $\underline{S}$ results for Si:P (Ref. 3). The true $S_c=1.915$ kbar (see dashed line) while the apparent $S_c^*=1.70$ kbar. An optimized forced fit to the data for $\sigma>6$ S/cm yields $S_c=1.915$ kbar and a scaling exponent $t=0.59$. The inset shows the calculated $\langle\sigma(\underline{S},T=0)$ from Eq. (14) vs $\underline{S}/S_c-1$ as the dashed line for the symmetric case $[z_1/L=0.30, z_2/L=0.70]$, yielding $t_{\rm eff}\sim 1.18$. A small asymmetry (2%) reduces the exponent to the $t\sim 1.0$ reported by WPL.

approximate fit to linear scaling with $t\sim 1$. WPL have reported $S_c=1.75$ kbar; however, this analysis suggests that the stress value 1.72 kbar in WPL's Fig. 1 yields $\sigma(T\rightarrow 0)\sim 0.27$ S/cm, which in turn from Fig. 2 suggests $S_c^*=1.70$ kbar. This small quantitative difference is not important to the correct understanding of the tail region. In this case the ratio of the true critical stress S_c to the apparent critical stress S_c^* is $1.915/1.70\sim 1.126$. This is closer to one than the BSB case where $S_c^*/S_c\sim 1.53$ $(S_c/S_c^*\sim 0.65)$. The WPL sample has a smaller L/a ratio (18.75) than the BSB case (26.66) and has a smaller value of λ_m and less than $\frac{1}{2}$ the SI from sample bending as for the BSB sample. However, the other critical difference in the two experiments is the much larger voltage electrode spacing for the WPL sample. With $z_2-z_1=0.4L$ for the WPL sample compared with $z_2-z_1=\frac{1}{8}L$ for the BSB sample the z integration yielding $\langle\sigma\rangle$ differs more from $t+1$ for the WPL case than for the BSB case. The integration of Eq. (7) yields the result shown in the inset in Fig. 3 with an effective exponent 1.18 for the symmetric case $(z_1=0.3L,\ z_2=0.7L)$. A small asymmetry of the voltage leads with respect to λ_m $(z_1=0.29L,\ z_2=0.69L)$ leads to an effective exponent near 1.0. This demonstrates that the effective exponent observed depends on three factors: (1) the SI from bending, (2) the spacing z_2-z_1 of the voltage leads, and (3) the asymmetry of the voltage leads with respect to the point of maximum deflection of the column.

$\langle\sigma\rangle/\sigma_0$ for the WPL electrode spacing has been calculated for four different values of the asymmetry versus $\underline{S}/S_c^*-1$ over a wider range of $\underline{S}/S_c^*-1$. The results (not shown) are similar to the BSB results in Fig. 2 and demonstrate the effective exponent varying with both $\underline{S}/S_c^*-1$ and the asymmetry. For very small values of $\underline{S}/S_c^*-1<0.001$ the exponent approaches again the original exponent $t=\frac{1}{2}$ just as in Fig. 2, but this regime is well beyond the experimental data.

III. DOPING INHOMOGENEITY

For a random distribution of donors (acceptors) in a host semiconductor with a concentration $N_d(\mathbf{r})$ we shall employ a probability distribution $P(N_d)$ characterized by a width χ such that for a homogeneous distribution $\chi=0$. In the most general case there will be correlation between dopant density $N_d(\mathbf{r})$ and $N_d(\mathbf{r}')$ characterized by a correlation function as a function $|\mathbf{r}-\mathbf{r}'|$. The general case is more difficult to treat and the nature of the correlation function is often not known. It would be particularly difficult to treat the case of dopant striations found in some thermally doped samples. To obtain an idea of the effect of DI on the critical behavior of transport we shall start with the simple case of totally correlated DI analogous to the stress case discussed above.

A. Correlated case

A linear variation of the doping $n(y,z)$ across the cross section of a rectangular bar $[a<b, -b/2<y<b/2]$ of length L can be treated exactly. The doping variation in the x direction $[-a/2<x<a/2]$ will be neglected. When the average doping is $\underline{n}$ at the center $[x=y=z=0]$ of the sample section between the two voltage electrodes at z_1 and z_2 the doping $n(y,z)=\underline{n}(1+gy+hz)$, where g and h are constants, one finds for $\sigma(n)=\sigma_0(n/n_c-1)^t$ that the integral over a cross section at fixed z yields

$$\sigma(z)=\sigma_0\int_{y^*}^{b/2}dy[n(y,z)/n_c-1]^t$$
$$=[\sigma_0/bg(t+1)][\underline{n}/n_c(1+gb/2+hz)-1]^{t+1}, \quad (8)$$

where the lower limit y^* is determined by the condition $n_c=\underline{n}(1+gy^*+hz)$, which guarantees that the lower limit makes a zero contribution to the integration. $\sigma(z)$ varies along the z axis and has its smallest value for g and h positive at $z_1=-\Delta/2$. The ''pinchoff'' point $[\rho(z)=1/\sigma(z)\rightarrow\infty]$ leads to the minimal value of $\underline{n}_{\rm min}$ given by

$$\underline{n}_{\rm min}=n_c/(1+gb/2-hz_1). \quad (9)$$

Ordinarily experiments are performed with a constant current and the voltage between the two electrodes is measured, thus determining the resistance between the two electrodes. This resistance $R=(1/ab)(1/(z_2-z_1)\int_{z1}^{z2}\rho(z)dz$ and in turn leads to an average conductivity $\langle\sigma(z)\rangle_{\rm expt}=(z_2-z_1)/\int_{z1}^{z2}dz/\sigma(z)$. This result differs from a straight average $\sigma(z)$ of the form $(z_2-z_1)^{-1}\int_{z1}^{z2}\sigma(z)dz$, although the difference is small when z_2-z_1 is small enough. The ''pinchoff'' point at $\underline{n}_{\rm min}$ in Eq. (8) corresponds to the apparent critical density n_c^* resulting from DI. Numerical calculations have been made for several values of g and h of the critical behavior of $\langle\sigma(z)\rangle_{\rm expt}$ versus (n/n_c^*-1). These results are shown in Fig. 4.

The case of a pure longitudinal z variation $(g=0, h\neq 0)$ of $n(z)$ and $\sigma(z)$ with no variation in the transverse direction

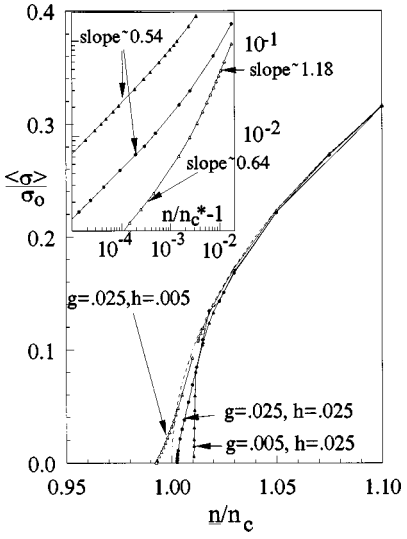

FIG. 4. Effect of a linear DI on the critical behavior of $\langle\sigma\rangle/\sigma_0$ vs $\underline{n}/n_c$ for three different linear dopant variations $n(y,z)=\underline{n}(1+gy+hz)$ [△, $g=0.025$, $h=0.005$; ●, $g=0.025$, $h=0.025$; ▲, $g=0.005$, $h=0.025$]. The apparent n_c^* can be shifted either up or down depending on the ratio of h/g. When the linear DI is mostly transverse ($h/g \ll 1$), n_c^* is pushed below n_c and the exponent t_{eff} is increased above the result $t=\frac{1}{2}$ for zero DI. The inset shows $\langle\sigma\rangle/\sigma_0$ vs $\underline{n}/n_c^*-1$ very close to n_c^*. The results show the scaling approaching the exponent 0.54 close to the original $t=\frac{1}{2}$. Very close to n_c^* the integral $\int\rho(z)dz$ is dominated by the peak at $z=z_1$ as in the case in Fig. 1.

deserves special mention. In this case $\langle\rho\rangle=[1/\sigma_0(z_2-z_1)]\int dz/[(\underline{n}/n_c)(1+hz)-1]^{1/2}$. Unlike the case with a transverse variation, $\langle\rho\rangle$ does not diverge as $n\rightarrow n_{\min}/(1-hz_1)$. Although it is unlikely to have such a case with a pure z variation, the result is similar to an extreme case of one result observed by Rosenbaum *et al.*[33] in their high-resolution uniaxial stress experiment in which for this case $\sigma(\underline{S},T)$ appears to remain above 5 S/cm as $\underline{S}/S_c-1$ approaches -0.4. However, it would be difficult to convincingly claim that there was no transverse variation of S in a compressive uniaxial stress experiment.

B. Uncorrelated doping inhomogeneity

Consider a normalized distribution $P(N_d(\mathbf{r}))=C\exp\{-[(N_d-\underline{N}_d)/\chi n_c]^2\}$ where $C=(\sqrt{\pi}\chi n_c)^{-1}$. As $\chi\rightarrow 0$, $P(N_d)$ approaches a δ function. It is straightforward to demonstrate that

$$\chi=(2/3)^{1/2}\{\langle[(N_d-\underline{N}_d)/n_c]^2\rangle\}^{1/2}. \tag{10}$$

For a homogeneous case the critical behavior of the conductivity can be represented by $\sigma(n,T\rightarrow 0)=\sigma_0|n/n_c-1|^t$ where for uncompensated systems $n=N_d$ and n_c is the critical density. The scaling exponent t will depend on the system involved and the type of transport process. For variable-range hopping (VRH) the theoretical prediction yields $t=3$ for the Mott VRH prefactor. For $n>n_c$ the scaling of metallic samples such as crystalline Si:P or Ge:Ga yields $t=\frac{1}{2}$, while for a wide range of amorphous $Si_{1-x}M_x$ and $Ge_{1-x}M_x$ alloys one finds $t\sim 1$. In the limit that χ is very small and one is not to close to the critical point [$\sigma(n)$ large], $P(n-\underline{n})$ acts as a δ function and $\langle\sigma\rangle=\sigma_0\int|n/n_c-1|^t\delta(n-\underline{n})dn=\sigma_0|\underline{n}/n_c-1|^t$. The corrections because $P(n-\underline{n})$ is not a δ function are of the form

$$\langle\sigma\rangle=\sigma_0|\underline{x}|^t[1+O(\chi\underline{n}/n_c\underline{x})^2+O(\chi\underline{n}/n_c\underline{x})^4+\cdots], \tag{11}$$

where $\underline{x}=|\underline{n}/n_c-1|$. The first correction is proportional to χ^2 and is small as long as $\underline{n}$ is not near the critical point n_c. When t is an integer an exact result can be obtained when the lower limit is extended to $-\infty$ since the integral $\int_{-\infty}^{+\infty}x^t\exp[-(x-\underline{x})^2/\chi^2]$ yields a Hermite polynomial $H_t(i\underline{x}/\chi)$. Thus, for t an integer, one explicitly obtains

$$\langle\sigma\rangle=\sigma_0[\underline{x}^4+3\chi^2\underline{x}^2+3/4\chi^4] \quad \text{for } t=4, \tag{12a}$$

$$\langle\sigma\rangle=\sigma_0[\underline{x}^3+3/2\chi^2\underline{x}] \quad \text{for } t=3,$$

$$\langle\sigma\rangle=\sigma_0[\underline{x}^2+1/2\chi^2] \quad \text{for } t=2, \tag{12b}$$

and $\langle\sigma\rangle=\sigma_0\underline{x}$ for $t=1$. The last result for $t=1$ is significant because it demonstrates that an uncorrelated DI of the Gaussian form has no effect on the scaling exponent, even though there may be a change in the critical density n_c to an apparent critical density n_c^*. For odd values of $t>1$, $\langle\sigma\rangle\rightarrow 0$ as $\underline{x}\rightarrow 0$, while for even values of t, $\langle\sigma\rangle\rightarrow\text{const}\times\chi^t$. For non-integer values of $t>1$, $\langle\sigma\rangle\rightarrow\text{const}$ as $\underline{x}\rightarrow 0$. This result qualitatively explains the density dependence of the prefactor $\sigma_0(n)$ n dependence for Mott VRH as $n\rightarrow n_{c-}$ as discussed previously.[34]

A particularly important case for the metallic side of the MIT is the case $t=\frac{1}{2}$. Here the integration yields [using Gradsteyn and Rhyzik's (3.462)]

$$\langle\sigma\rangle=\sigma_0(\sqrt{\chi}/2^{7/4})\exp\{-(\underline{x}^2/2\chi^2)\}D_{-3/2}(\sqrt{2}(1-\underline{n}/n_c)/\chi), \tag{13a}$$

where

$$D_{-3/2}(z)=(1/2^{3/4})\exp[-(z^2/4)]\times\{[\sqrt{\pi}/\Gamma(5/4)]\Phi(3/4,1/2,z^2/2)-[\sqrt{\pi}/\Gamma(3/4)]\Phi(5/4,3/2,z^2/2)\}, \tag{13b}$$

where $z=\sqrt{2}(1-\underline{n}/n_c)/\chi$. The cylinder function $D_{-3/2}(z)$ involves the difference of two hypergeometric functions. Doing the series expansion of these [$\Phi(3/4,1/2,x)=1+3/2x+7/8x^2$, $\Phi(5/4,3/2,x)=1+5/6x+3/8x^2$] and keeping only the first terms in the expansion $\langle\sigma\rangle$ becomes

$$\langle\sigma\rangle=\sigma_0(\sqrt{\chi}/2^{5/2})\exp[-(\underline{x}/\chi)^2][(\sqrt{\pi}/\Gamma(5/4)+2\sqrt{\pi}/\Gamma(3/4)(\underline{x}/\chi)+O(\underline{x}^2/\chi^2)+\cdots]. \tag{14}$$

This result is only valid with the first few terms for small values of $\underline{x}$ such that $\underline{x}/\chi<1$. For large values of $\underline{x}$ and $\langle\sigma\rangle$ very large $P(n-\underline{n})$ behaves like a δ function and the scaling behavior is characterized by $t=\frac{1}{2}$. For $\underline{x}=0$, Eq. (5) yields $\langle\sigma\rangle=\sigma_0(\sqrt{\pi}\sqrt{\chi}/2^{5/2}\Gamma(5/4))\sim\sigma_0\sqrt{\chi}/3$. The conductivity at the true critical point is proportional to $\sqrt{\chi}$ and is therefore a

direct measure of the DI. Keeping only the first two terms in Eq. (5) for the regime $\underline{x}/\chi<1$, one obtains

$$\langle\sigma\rangle\approx\sigma_0\{(\pi\chi)^{1/2}\Gamma(3/4)/2^{7/4}\Gamma(5/4)[2\Gamma(5/4) - \Gamma(3/4)]\}(\underline{n}/n_c^*-1), \tag{15a}$$

where

$$n_c^*\approx n_c\{1-(\chi/2)[\Gamma(3/4)/\Gamma(5/4)]\}\sim n_c(1-0.67\chi). \tag{15b}$$

From Eq. (6) the effect of DI for the important $t=\frac{1}{2}$ case is to shift the observed critical density down an amount proportional to the DI. However, the scaling behavior measured with respect to the apparent critical density n_c^* is linear with an apparent scaling exponent $t^*\sim 1$. The DI leads to a crossover between the true scaling exponent of $t=\frac{1}{2}$ for larger values of $\underline{x}$ to the apparent scaling exponent $t^*=1$ when $\underline{x}/\chi<1$. The smaller the value of χ, the smaller the value of $\langle\sigma\rangle$ where the crossover takes place. However, it is not a good approximation to keep only two terms in Eq. (14). When a large number of terms is kept there is not a sharp cutoff of $\langle\sigma\rangle$ at some particular value of n_c^* and there is a long tail. Nevertheless, a broad distribution (χ of order unity) destroys any semblance of scaling of $\langle\sigma\rangle$ with a scaling exponent $\frac{1}{2}$.

The symmetrical Gaussian distribution is not a good approximation for the a-Si:M and a-Ge:M alloys. In these cases the conductivity prefactor σ_0 is the same order of magnitude as for Si:P and Si:As despite the fact that the *doping density itinerant carrier density is three orders of magnitude larger than for Si:P and Si:As*. A simple explanation for this is that there is a broad distribution $P((n-\underline{n})/n_c))$ for these a-semiconductor-metal alloys. A particularly simple broad distribution linear in $(n-\underline{n})/n_c$ is of the form $P(n-\underline{n})=a+b(n-\underline{n})/n_c$ such that $\int_{-\ell}^{+\ell}P(n-\underline{n})dn/n_c=1=2a\ell$. This leads to a conductivity $\sigma(\underline{n})=\sigma_0\int_0^3 x^{1/2}[a+b(x-\underline{x})]dx$ where $\underline{x}=\underline{n}/n_c-1$ and the upper limit of 3 is for $x_c=0.25$. The integral leads to the result

$$\langle\sigma(\underline{n})\rangle=2\sqrt{3}\sigma_0[a+2.8b-b(\underline{n}/n_c)]. \tag{16}$$

The experimental results for various a-semiconductor-metal alloys suggest $\sigma(\underline{n})$ at $T=0$ scales to zero for $\underline{n}/n_c=\mu$ with $0.4<\mu<0.56$, which is close to but slightly smaller than the Zallen-Scher criterion. Equation (16) then yields $b=-a/(2.8-\mu)$ and

$$\langle\sigma(\underline{n})\rangle=[2\sqrt{3}\mu\sigma_0/2\ell(2.8-\mu)](\underline{n}/n_c^*-1), \tag{17}$$

where

$$n_c^*/n_c=\mu.$$

For $\mu=\frac{1}{2}$ the effective prefactor is $0.75\sigma_0/2\ell$, demonstrating that it is inversely proportional to the width of the distribution $P(n-\underline{n})$. This broad linear distribution converts the scaling exponent from $\frac{1}{2}$ in the absence of DI to 1 and yields a much smaller effective prefactor. For this case there is no remnant of the scaling exponent $\frac{1}{2}$ left in $\langle\sigma(\underline{n})\rangle$. Even though the intrinsic exponent of $\frac{1}{2}$ resulting from ionized impurity scattering is like that for Si:P, etc., it is removed by a broad distribution $P(n-\underline{n})$. Whether this distribution $P(n-\underline{n})$, given by

$$P(n-\underline{n})=(1/2\ell)\{1-[1/(2.8-\mu)][(n-\underline{n})/n_c]\}, \tag{18}$$

is a realistic distribution is a difficult question to answer and will be discussed more in the Discussion. It becomes small for $(n-\underline{n})/n_c$ larger than 2, but becomes negative for $(n-\underline{n})/n_c>(2.8-\mu)$. Physically, $P(n-\underline{n})$ must be positive: however the negative portion represents only a few percent of the normalized distribution and will not change the fact that this broad, linear distribution can explain the scaling exponent 1, when the intrinsic exponent for the homogeneous system is $\frac{1}{2}$. If $t=1$ for the homogeneous case, the above analysis changes slightly and still yields $\langle\sigma(\underline{n})\rangle\propto(\underline{n}/n_c^*-1)$ with $n_c^*=\mu n_c$. A constant distribution, such as that for SI in Eq. (2), can be treated for the $t=1$ case and leads to results analagous to those in Sec. II, but is not able to explain the scaling exponent.

An effort has been made to fit the conductivity $\sigma(\underline{n},T=0)$ employing an asymmetrical Gaussian of the form

$$P(n-\underline{n})=C\exp-[(n-\underline{n})/\chi n_c]^2[1+b(n-\underline{n})/\chi n_c], \tag{19}$$

where the normalization coefficient $C=(1/\sqrt{\pi}n_c\chi)$ for the symmetrical Gaussian distribution and the correction term introducing the asymmetry can be varied by varying b. Introducing the quantities $x=(n/n_c-1)$, $\underline{x}=(\underline{n}/n_c-1)$, $y=\sqrt{2}x/\chi$, and $z=(\sqrt{2}/\chi)(1-\underline{n}/n_c)$, one has $(n-\underline{n})/n_c\chi=(y+z)/\sqrt{2}$. Here $\langle\sigma(\underline{n})\rangle$ becomes

$$\langle\sigma(\underline{n})\rangle=\sigma_0(\chi/4\pi)^{1/2}\exp(-z^2/2)\int_0^{Y_c}y^{1/2}\exp(-y^2/2)\exp(-yz)[1+b'(y+z)]. \tag{20}$$

The upper limit $y_c=(\sqrt{2}/\chi)x_c$, where $x_c=n_{\max}/n_c-1$. For a percolation threshold of 0.25 for continuous percolation one expects $x_c=3$ and y_c is determined by the breadth χ of the Gaussian. Equation (20) is evaluated as a power series in z by employing a Taylor series expansion of e^{-yz} and a numerical evaluation of the integrals $\int_0^{Y_c}y^{1/2+n}\exp(-y^2/2)dy$ for $n=0-12$ for a series of different cutoffs y_c from 2 to 6 and for b' values from -0.8 to $+0.8$. Figure 5 shows $\sigma(z)$ versus z [$z\propto-(\underline{n}/n_c-1)$] for $y_{\text{cutoff}}=6$ for a range of b values. All of the curves show a linear region (within 7%), as large as a factor of 6. The bendover at large values of $\sigma(z)$ is well beyond the experimental data ($n>2n_c^*$), but the tail at small values of $\sigma(z)$ is inconsistent with the experimental data for a-$Si_{1-x}Nb_x$, etc. Typical experimental data show a linear behavior over a factor of 10–20. There is a relationship between the parameter b and the cutoff z_c, and also n_c^*/n_c is given by $1-(x_c/y_c)z_c$. Based on the data, the continuous percolation limit $p_c\approx 0.25$, and the Zallen-Scher criterion, one expects $n_c^*/n_c\sim 0.5$, which is given for $y_c=6$ by $z_c\sim 1$, leads to $b\sim 0.26$. If one reduces y_c (equivalent to increasing χ and broadening the distribution) to 4, this re-

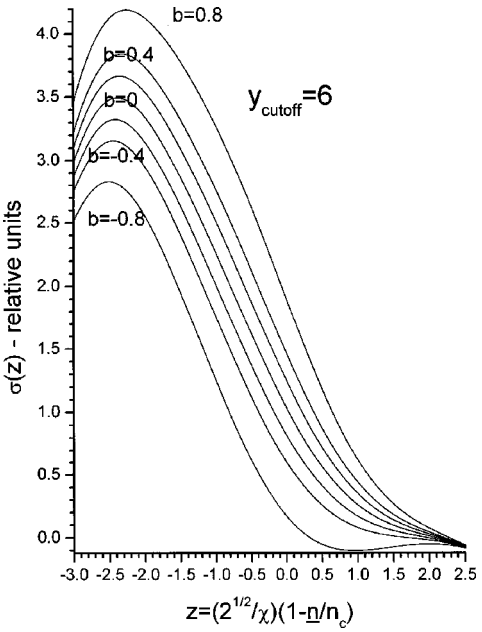

FIG. 5. $\langle\sigma(z)\rangle$ vs z for an asymmetrical Gaussian (when the scaling exponent is $t=\frac{1}{2}$ in the absence of DI) with an upper cutoff y_{cutoff} for values of b' equal to -0.8, -0.4, -0.2, 0, 0.2, 0.4, 0.8. The linear region (within 7%) varies between 4.5 and 6 as a function of b. The cutoff z_{cutoff} is determined from the extrapolation of the linear region to $\langle\sigma(z_{\text{cutoff}})\rangle=0$. The asymmetrical Gaussian is not able to explain scaling with $t\sim1$ with a factor of 10–20 in σ.

duces z_c to 0.7 and reduces b to near 0. Reducing b reduces the tail of $\sigma(z)$, but the tail cannot be totally eliminated.

The asymmetrical Gaussian distribution with a cutoff x_c (and y_c) totally removes evidence of the $t=\frac{1}{2}$ scaling behavior for $\langle\sigma(\underline{n})\rangle$ when the distribution is broad enough, but is not able to produce a linear region over the factor of 10–20 required to explain the scaling exponent $t\sim1$ for the *a*-semiconductor-metal alloys.

IV. DISCUSSION

A. Temperature-dependent conductivity $\sigma(\underline{S},T)$ in the presence of stress inhomogeneity

This is particularly complicated on the insulating side of the transition ($\underline{S}<S_c^*$ for Si:P, $\underline{S}>S_c^*$ for Si:B) because there are three possible contributions to $\sigma(\underline{S},T)$ from Mott VRH, Efros-Shklovskii (ES) VRH, and activated conduction from carriers thermally excited above the mobility edge. For no SI, $\sigma(S,T)$ takes the form

$$\begin{aligned}\sigma(S,T)=&\sigma_{0,\text{act}}(S)(T/T_{0,\text{act}})^p\exp\{-[E_{\text{act}}(S,n)/kT]\}\\&+\sigma_{0,\text{Mott}}(n,S)[T_0(S,n)/T]^q\exp\\&\times\{-[T_0(S,n)/T]^{1/4}\}+\sigma_{0,\text{ES}}(S,n)[T_0'(S,n)/T]^r\\&\times\exp\{-[T_0'(S,n)/T]^{1/2}\},\end{aligned}\tag{21}$$

where each of the prefactors and exponentials can depend on the stress S and on the dopant density. The experimentally measured quantity $\langle\sigma\rangle$ in the presence of SI is an extremely complex quantity given by $\langle\sigma(\underline{S},T)\rangle=(z_2-z_1)/\int dz/\sigma(z,\underline{S},T)$. Evaluation of this integral depends on detailed knowledge of the S dependence of the prefactors and exponentials in Eq. (21) and is well beyond the scope of this discussion. BSB have argued that their data $[\langle\sigma\rangle\propto T^{1/2}\exp-(T_0'/T)^{1/2}]$ supported the dominance of ES VRH for $\underline{S}>S_c^*=613$ bars. However, no theoretical prediction for ES VRH supports an exponent $r=-\frac{1}{2}$. Efros and Shklovskii[35] obtain $r=+\frac{1}{2}$, and the same result has recently be obtained by Castner.[34] Furthermore, in the absence of both SI and DI the prefactor $\sigma_0(n)$ scales to zero as $n\rightarrow n_c$ as $1/\xi^3$, where $\xi=\xi_0(1-n/n_c)^{\nu}$ is the localization length and ν is the localization length exponent. An alternative explanation for the $T^{1/2}$ prefactor reported by BSB is that it arises from the prefactor of the activated conduction term. This same $T^{1/2}$ prefactor dependence has been demonstrated to be associated with the activated term in Eq. (21) for Si:As for insulating samples in the zero-stress case for $0.86<n/n_c<0.98$. The DI for the Si:As samples is small and is estimated at less than 2%, but even this small a DI can have a dramatic effect upon the prefactors of both the Mott and ES VRH prefactors as $n\rightarrow n_c$. There is also a new independent theoretical prediction[36] $\sigma(n=n_c,T)\propto(e^2/h)(2m^*kT/\hbar^2)^{1/2}$ based on classical ionized impurity scattering. This new $T^{1/2}$ contribution is in addition to the $m(n)T^{1/2}$ contribution of Altshuler and Aronov in the diffusion channel due to electron-electron interactions. This new classical contribution has the right magnitude to explain the BSB result $\langle\sigma(\underline{S}=S_c^*,T\rangle=7.6\sqrt{T}$ S/cm. However, any numerical comparison needs to take account of the large SI (>60%) in the BSB experiment because of sample bending. This large SI could readily account for a reduction in the magnitude of Mott VRH for $\underline{S}>S_c^*$, but one has to carefully account for the activated term resulting from carriers thermally excited above the mobility edge before concluding the dominant contribution to VRH results from the ES contribution. In the zero stress results the Mott VRH contribution is usually only dominant for $0.90<n/n_c<0.99$ for the doped Si results (Si:P, Si:As, and Si:B). However, it should be noted that for the NTD Ge:Ga samples Watanabe *et al.*[37] have demonstrated ES VRH is dominant for $0.90<n/n_c<0.99$. The NTD-prepared samples are acknowledged to be the most homogeneous of all samples (doped Si and Ge) studied to date.

B. Deflection from bending for nonideal compressive loaded columns

Ideal columns under compressive loads are unstable for pivoted or round ends against bending. Flat ends provide some stability, but when the ends are mounted in solder[1,2] or on cigarette paper,[3] the stabilizing effect of flat surfaces is dissipated. From the principle of virtual work one can calculate the deflection from the equation $\Delta(P\delta)=\Delta(\text{strain energy})$ where the stored strain energy consists of that due to bending $[U_{\text{bending}}=(EI/2)\int_0^L(d^2y/dz^2)^2dz]$ and a smaller shear component. P is the pressure load and δ is the displacement in the direction of the applied force PA. In any experimental situation the loading is not ideal because (1) there is an eccentricity of the forces at the two ends of the

sample, (2) the two sample end flats are not flat and perfectly parallel, (3) the load bearing surfaces are not rigid enough compared with the sample being compressed, and (4) the sample ends can displace small amounts in the solder. The deflection d_m at the midsection ($z=L/2$) of a column with an eccentricity e (of the parallel forces) is given[38] by

$$d_m=(4/\pi)e(\underline{P}/P_c)/(1-\underline{P}/P_c), \tag{22}$$

where P_c, the critical stress, is given by π^2EI/L^2 for a column of length L when the slenderness ratio is sufficiently large. However, it is also known for steel that for slenderness ratios L/r ($r^2A=I$, $r\equiv$radius of gyration) less than 100 P_c stops increasing with decreasing L/r and saturates at the yield point of the material. For the BSB sample, $L/r=92$. The yield points for B-doped and P-doped Si at low temperatures are not well characterized but might be expected to be lower than the Euler value. BBS (Ref. 31) have suggested a P_c of 24 kbar based on an Euler expression using $L/2$ as the effective length of the column. The correct Euler result for the BSB geometry is $\frac{1}{4}$ of this amount. It is worth noting that Rosenbaum[39] broke Si:P samples at 7 kbar. The result in Eq. (22) either suggests that for $d_m\sim e$ that one requires $\underline{P}/P_c\sim\frac{1}{2}$ or for $\underline{P}/P_c\ll 1$ requires $e\gg d_m$, or that there other sources of the bending. The presence of microcracks near the surface from sawing or grinding that were not totally removed by etching could also lead to a reduced value of P_c. Without more detailed knowledge of the yield point for doped Si and more detailed knowledge of the defects associated with the loading (distortion of the Be membrane) it is not possible to resolve this issue. However, the main point of Eq. (22) is that the deflection can increase linearly with $\underline{P}$ and, unlike the ideal case, is not negligible until $\underline{P}$ is very close to P_c. It is common laboratory experience that slender steel rules and wooden yard sticks can bend substantially at loads $\underline{P}\ll P_c$ under compression. *The SI due to bending under compression can be removed by performing careful experiments under tension*.

C. Uniaxial stress experiments in tension

Although the above analysis in Secs. II and III separately considers the role of SI and DI, the reality is that both are present simultaneously. In all three uniaxial stress experiments under compression[1–3] the SI is much larger than the DI ordinarily accounted for in high-quality doped Si ingots. The only possible exception to this is the one case reported in Ref. 33 where $\sigma(\underline{S},T\rightarrow 0)$ remains above 5 S/cm for small values of $\underline{S}$. All the other results yield a reasonably sharp value of the cutoff S_c^* where $\sigma(\underline{S}\rightarrow S_c^*,\ T=0)\rightarrow 0$. Even the WPL experiment with the smallest slenderness ratio L/a and the smallest bending deflection still shows S_c^* 12.6% less than S_c, which is a much larger change in the critical point than would be expected from DI, which is normally expected to be less than 2% and in the best quality samples may be of order or less than 0.5%. One would have to decrease the SI by a factor of 10 or more to make it less than the DI. This can be accomplished by decreasing $(L/a)^2$ by more than a factor of 10. This may be possible, but an alternative experimental solution is the use of tension in the uniaxial stress experiment rather than compression. Although most uniaxial stress experiments have been done in compression, there are at least two cases where tension has been successfully employed. The first by Watkins and Ham[40] studied the removal of the orbital degeneracy of the Li donor in Si by uniaxial stress. The second is a piezocapacitance study[41] of doped Si:P and Si:Sb. Neither of these studies were near the critical regime for the onset of metallic behavior at $T=0$. A carefully executed tension study in the critical regime of $\sigma(S,T\rightarrow 0)$ should resolve any doubts about the role of SI.

D. Doping Inhomogeneity results

The uncorrelated case with a Gaussian distribution $P(N_d)$ of donors about an average value $\underline{N}_d$ always yields a reduction in the critical density given by $(n_c-n_c^*)/n_c=0.63\chi$ and is 0.51 times the rms dopant deviation from the average value $\underline{N}_d$. A 4% rms dopant deviation leads to a 2% reduction in n_c. For metallic samples with a scaling exponent $t=\frac{1}{2}$ in the absence of DI there can be a crossover to an effective exponent $t^*=1$ when $\underline{N}_d$ is sufficiently close to n_c^* from compensation. On the other hand, if $t=1$, there will be no change in the exponent even though n_c^* is reduced below n_c by the DI. For amorphous semiconductor-metal alloys the true x_c will be reduced to x_c^* by DI.

The effects of correlated linear doping variations of the form $n(y,z)=\underline{n}(1+gy+hz)$, where $\underline{n}$ is the average dopant density at the center of the sample region between the voltage electrodes at z_1 and z_2, are demonstrated in Fig. 4 showing $\langle\sigma\rangle/\sigma_0$ versus $\underline{n}/n_c$ when $t=\frac{1}{2}$ (see dashed line for zero DI) for three different values of (g,h). When to DI is predominantly transverse ($g=0.025$, $h=0.005$, symbol $\triangle$) the results show a reduction of n_c to n_c^* of 0.75%. The scaling exponent increases when $\underline{n}/n_c<1.01$ and is in the vicinity of 1.18 for $\underline{n}/n_c^*-1\sim 0.01$. However, as shown in the inset for even smaller values of $\underline{n}/n_c^*-1<10^{-3}$ the effective exponent t^* reverts toward a smaller value. When the DI in the y and z directions is equal ($g=0.025$, $h=0.025$, symbol $\bullet$) there a very small *increase in* n_c of 0.25% and only a small increase in the exponent t^*. The inset shows the exponent $t^*\sim 0.54$ for $\underline{n}/n_c^*-1<3\times 10^{-4}$. In the third case for the DI 5 times greater in the z direction than in the y direction ($g=0.005$, $h=0.025$, symbol $\blacktriangle$) the increase in n_c is 1.06% and the effective exponent increases only a small amount that would be observable near $\underline{n}/n_c^*-1\sim 0.01$, but is close to 0.54 for $\underline{n}/n_c^*-1<10^{-3}$. Unlike the uncorrelated case, n_c^* can be either less or greater than n_c dependent on the geometry of the DI. Likewise, the effective exponent does not show a universal change, but depends on the geometry of the DI. A transverse DI favors an increase in t^*, but only in a limited range of $\underline{n}/n_c^*-1$. A surprising case result for a pure longitudinal DI ($g=0, h\neq 0$) for the $t=1/2$ case is the absence of a true critical point where $\sigma(\underline{n}\rightarrow n_c^*,T=0)\rightarrow 0$. This is readily demonstrated by the integration of $\rho(z)$ between the voltage electrodes at z_1 and z_2. However, the probability of the pure longitudinal case occuring with $g=0$ is negligible.

TABLE I. Room temperature resistivity angular variation of Si:As

Sample	$\langle\rho_{RT}\rangle$ ($\times 10^{-3}$ Ω cm)	N_d ($\times 10^{18}$/cm^3)	$\langle(\rho-\langle\rho\rangle)^2\rangle^{1/2}$ ($\times 10^{-3}$ Ω cm)	rms/$\langle\rho\rangle$
$B'2$	8.15	7.75	0.166	0.021
$E14$	7.09	9.40	0.139	0.020
$D14$	6.99	9.50	0.039	0.0056
$A2$	3.24	22.0	0.038	0.0116

There are several ways to experimentally determine the macroscopic DI. Experimentalists ordinarily profile semiconductor wafers cut from ingots. This yields a resistivity profile at room temperature (RT) across a typical 5-cm-diam wafer. However, the voltage electrode spacing of samples with welded $Au_{0.98}Sb_{0.02}$ wire is comparable to the probe spacing of a four-point probe. As a result, it is not possible to accurately determine the DI for a length scale z_2-z_1. A determination of the transverse DI for a slender bar sample employed in typical studies is not possible with conventional resistivity probes. With the van der Pauw geometry samples it is possible to obtain information of the asymmetry resistance ratio R_1/R_2, where R_1 and R_2 are the resistances at right angles to each other. The Hall results[42] for Si:As demonstrated R_1/R_2 ratios near unity, but in the worse cases as large as 2 and as small as 0.4. This asymmetry leads to a well-known correction to the resistivity for a disk given by the asymmetry correction factor $f(x)=1-(\ln 2/2)x^2-O(x^4)$ where $x=(R_1-R_2)/(R_1+R_3)$. The ratios R_1/R_2 do not permit reliable quantitative estimates of the inhomogenity for bar-shaped samples, even though they tell us which samples have larger DI. Another approach for disk-shaped samples is the measurement with the four-point probe at RT of ρ as a function of the angle θ with respect to a fixed reference line in the disk. Typical results for three metallic and one insulating Si:As samples are shown in Table I $\rho(\theta)$ was measured at $\theta=n(\pi/4)$ with $n=0-7$. The results show fractional rms deviations ranging from 0.5% to 2%. All the Si:As disk-shaped samples show angular variations in this range. None of the samples from this ingot gave indications of striations in the resistivity, although disk-shaped samples from another supplier did give evidence of striations. The results in Table I were used as an estimate of possible linear variations of DI and the calculated results of DI presented in Fig. 4. Trappmann *et al.*[43] employed scanning tunneling microscopy to study Si:P samples with N_d up to 7×10^{19}/cm^3 and found no evidence of clustering and obtained a good fit to a Poisson distribution of donors.

E. Uncorrelated doping inhomogeneity

It is important to understand why the scaling exponent $t\approx1/2$ for Si:P is observed very close to the critical density $(\underline{n}/n_c-1)<10^{-3}$ when the donor distribution obeys Poisson statistics. Poisson statistics features large short-range disorder. From the vantage point of itinerant electrons the Poisson distribution (approximated by a Gaussian) appears sharper and sharper as $n\rightarrow n_{c+}$. The size of the itinerant electron wave packets with wave vectors near k_F, as determined by the Heisenberg uncertainty principle, is given by $\Delta x\Delta k>1$ where $\Delta k_{rms}\sim\beta k_F=2\pi\beta/\lambda_{dB}$ and $\Delta x_{rms}>\lambda_{dB}/2\pi$. The characteristic volume V_c associated with a wave packet near k_F is of order $(\lambda_{dB}/2\beta\pi)^3$. Although β is not reliably known for the random potential $V_{rp}(\mathbf{r})$, we will assume as a worst case that it is of order unity, although it might be as small as 0.1. Suppose we consider the Si:As case with $n_c=8.6\times10^{18}$/cm^3. For $\underline{n}=2n_c$, $k_F=4.4\times10^6$ cm^{-1}, and $\beta=0.5$, one finds, using $1/\chi=n_cV_c/10$ and $\chi=12$ corresponding to a rather broad distribution, probably too broad. However, for $\underline{n}=1.01n_c$, k_F decreases by 10 and V_c increases by 1000, leading to $\chi=0.012$. Even though the magnitude of these numbers is uncertain, the results show χ decreasing by a factor of 1000 from $2n_c$ to $1.01n_c$. It is this dramatic apparent sharpening of $P(n-\underline{n})$ seen by the itinerant electrons as $n\rightarrow n_{c+}$ that explains why the short-range disorder is unimportant as one approaches the critical point. The large wave packets of order $\lambda_{dB}(\underline{n})$ are simply not sensitive to the strong short-range fluctuations in $V_{rp}(\mathbf{r})$ and $P(n-\underline{n})$ acts like a delta function $\delta(n-\underline{n})$. For the Si:P and Ge:Ga cases one observes the scaling exponent $\frac{1}{2}$ quite accurately for both the furnace-grown samples and the NTD Ge:Ga samples. Even though Ge:Ga may obey a random distribution (Poisson statistics) better than Si:P, the difference in the scaling exponents is small because the itinerant electrons just above n_c are not sensitive to differences in the distribution $P(n-\underline{n})$ on a scale much less than $\lambda_{dB}(\underline{n})$.

How does this notion apply to a-$S_{1-x}M_x$ alloys like a-$Si_{1-x}Nb_x$? The distribution function $P(n-\underline{n})$ is likely to be very different than a Poisson distribution for Si:P where the probability of two P atoms on adjacent Si atoms is negligible. For the diamond lattice with $0.115=x_c<x<2x_c$ (a-$Si_{1-x}Nb_x$) there is a significant probability of adjacent M atoms and one expects two to three M atoms in the next-nearest-neighbor shell. This suggests the band structure will differ significantly from crystalline Si. The six valleys of the conduction band for the crystalline case probably do not survive. Alloy theory for disordered alloys involves the bond energies U_{SS}, U_{MM}, and U_{SM} and an energy difference $2U_{SM}-U_{SS}-U_{MM}$. Here the deposited films are likely to be well below the temperature for any long-range disorder transition and will be in a metastable state. However, the short-range order will still be important. For a single-valley conduction band $k_F\sim5.5\times10^7$ at $2x_c$ and $\lambda_{dB}\sim11$ Å. As compared with the Si:P case the characteristic volume $V_c\sim(\lambda_{dB}/2\beta\pi)^3$ containing less than one M atom and for $\beta=\frac{1}{2}$ leads to a $\chi\sim72$, which suggests a very much broader distribution than for Si:P. This is consistent with the small prefactor of $\langle\sigma(\underline{n})\rangle$ in Eq. (17). If one tries to explain the magnitude with the Wegner scaling expression $\sigma=(e^2/2\hbar\xi_0)(x/x_c-1)$ for a-$Si_{1-x}Nb_x$ (prefactor 300 S/cm) leads to $\xi_0\sim42$ Å. This is not a sensible magnitude for a correlation length for a-$Si_{1-x}Nb_x$. If one attempts to apply the Boltzmann expression at $2x_c$, one finds a small mobility $\mu\sim0.3$ cm^2/V/sec, which leads to a mean free path $\ell\sim2.3$ Å, which is less than the M-M atom spacing, but the same order as the Si-Si bond length. If one uses the expres-

sion $\sigma \sim (e^2/2\hbar)k_F(2x_c)$ for the prefactor based on the ionized impurity scattering, one will obtain a result a factor of 10 too large. If one uses Eq. (17), one can account for the prefactor with a $\underline{P}(n-n)$ width $2\ell \sim 6$. Although this explanation is speculative, there is every reason to believe that ionized-impurity-scattering (IIS) at low T will be the dominant scattering mechanism for the a-$S_{1-x}M_x$ alloys. This situation provides evidence for a broad distribution $P(n-\underline{n})$ for these systems, but the shape of the distribution cannot be convincingly established from the transport data alone. Since the a-$S_{1-x}M_x$ alloys do not exhibit the percolation exponent 1.6, unlike Na_xWO_3; one needs to understand the microscopic differences between these two MIT systems. In Na_xWO_3 the Na atoms are in interstitial sites of the WO_3 lattice and form metallic clusters. The M atoms in the a-$S_{1-x}M_x$ alloys are assumed to be substitutional and the distribution in Eq. (18) suggests an anticlustering tendency, but this has not been established from experimental evidence.

V. CONCLUSIONS

SI from sample bending is basically a perfectly correlated case with the transverse variation in S dominant. Far from S_c, SI provides only a small correction to $\sigma(\underline{S}, T=0)$; however, close to the critical point there can be a significant tail with an apparent S_c^* and an increase in the exponent from t to $t+1$ when $(z_2-z_1)/L$ is small. The detailed integration [Eq. (7)] allows a satisfactory explanation of the tail behavior observed by PRTB, BSB, and WPL. The integration over z of Eq. (7) explains the exponent 1.6 obtained by BSB and the exponent 1.0 obtained by WPL, the difference resulting from the different magnitudes of z_2-z_1/L. The correlated SI results from small sample bending. Performing uniaxial stress experiments in tension should remove the SI. Far enough from the critical point the PRTB, BSB, and WPL experimental results all support the scaling exponent $t=\frac{1}{2}$, which can be explained by ionized impurity scattering.

Correlated DI behaves in much the same manner as SI. Linear correlated DI can either increase or decrease n_c and can increase the scaling exponent t above $t=\frac{1}{2}$ when the linear DI has a significant transverse component. Some RT resistivity results for Si:As disks show fractional rms deviations of 0.5%–2.0%. Just as in the correlated SI case, a broad distribution $P(n-\underline{n})$ can mask the scaling exponent $t=\frac{1}{2}$ (of the homogeneous system) and lead to an exponent $t \sim 1$ for the correct shape of $P(n-\underline{n})$. This provides the plausible, but speculative notion that the physics of the transport at the microscopic level can be the same for both crystalline-doped semiconductors and the a-$S_{1-x}M_x$ alloys and the scattering for both cases is dominated by ionized impurity scattering. There is evidence that the a-$S_{1-x}M_x$ cases are characterized by a broad distribution $P(n-\underline{n})$. The size of the itinerant electron wave packet increases as the de Broglie wavelength $\lambda_{dB}(\underline{n})$ as $n \to n_{c+}$ and the effective Poisson distribution appears sharper approaching n_c. As $n \to n_c$, the itinerant electrons become increasingly insensitive to the short-range disorder.

ACKNOWLEDGMENTS

The author thanks K.J. Song for the room-temperature resistivity measurements of various Si:As samples as a function of angle. This work was partially supported by NSF Grant No. DMR-9803969.

[1] M. A. Paalanen, T. F. Rosenbaum, G. A. Thomas, and R. N. Bhatt, Phys. Rev. Lett. **48**, 1284 (1982); G. A. Thomas, M. A. Paalanen, and T. F. Rosenbaum, Phys. Rev. B **27**, 3897 (1983).
[2] S. Bogdanovich, M. P. Sarachik, and R. N. Bhatt, Phys. Rev. Lett. **82**, 137 (1999).
[3] S. Waffenschmidt, C. Pfleiderer, and H. v. Löhneysen, Phys. Rev. Lett. **83**, 3005 (1999).
[4] C. Castellani, G. Kotliar, and P. A. Lee, Phys. Rev. Lett. **59**, 323 (1987).
[5] P. Dai, Y. Zhang, and M. P. Sarachik, Phys. Rev. Lett. **67**, 136 (1991).
[6] P. Dai, Y. Zhang, S. Bogdanovich, and M. P. Sarachik, Phys. Rev. B **48**, 4941 (1993).
[7] D. K. Wilson and G. Feher, Phys. Rev. **124**, 1068 (1961).
[8] R. L. Aggarwal and A. K. Ramdas, Phys. Rev. **137**, A602 (1965); **140**, A1246 (1965).
[9] C. S. Smith, Phys. Rev. **94**, 42 (1954).
[10] F. J. Morin, T. H. Geballe, and C. Herring, Phys. Rev. **105**, 525 (1957).
[11] M. Pollak, Phys. Rev. **111**, 798 (1958).
[12] J. E. Aubrey, W. Gubler, T. Henningsen, and S. M. Koenig, Phys. Rev. **130**, 1667 (1963).
[13] O. N. Tufte and E. L. Stelzer, Phys. Rev. **133**, A1705 (1964).
[14] M. Cuevas and H. Fritzsche, Phys. Rev. **137**, A1847 (1965); **139**, A1628 (1965).
[15] G. L. Bir and G. E. Pikus, *Symmetry and Strain-Induced Effects in Semiconductors* (Wiley, New York, 1974).
[16] M. H. Cohen and J. Jortner, Phys. Rev. Lett. **30**, 699 (1973).
[17] N. F. Mott, Phys. Rev. Lett. **31**, 466 (1973).
[18] S. Kirkpatrick, Rev. Mod. Phys. **45**, 574 (1973).
[19] I. Webman, J. Jortner, and M. H. Cohen, Phys. Rev. B **11**, 2885 (1975); **13**, 713 (1976).
[20] H. Scher and R. Zallen, J. Chem. Phys. **53**, 3759 (1970); R. Zallen and H. Scher, Phys. Rev. B **4**, 4771 (1971).
[21] A. S. Skal, B. I. Shklovski, and A. L. Efros, Zh. Eksp. Teor. Fiz. Pis'ma Red. **17**, 522 (1973) [JETP Lett. **17**, 377 (1973)].
[22] P. A. Lightsey, Phys. Rev. B **8**, 3586 (1973).
[23] F. Wegner, Z. Phys. B **25**, 327 (1976).
[24] E. Abrahams, P. W. Anderson, D. C. Licciardello, and T. V. Ramakrishnan, Phys. Rev. Lett. **42**, 673 (1979).
[25] B. W. Dodson, W. L. McMillan, J. M. Mochel, and R. C. Dynes, Phys. Rev. Lett. **46**, 46 (1981).
[26] G. Hertel, D. J. Bishop, E. G. Spencer, J. M. Rowell, and R. C. Dynes, Phys. Rev. Lett. **50**, 743 (1983).

[27] N. Nishida, T. Furubayashi, M. Yamaguchi, M. Shinohara, Y. Miura, Y. Takano, K. Morigaki, H. Ishimoto, and K. Ono, J. Non-Cryst. Solids **59,60**, 149 (1983).
[28] S. Katsumoto, J. Phys. Soc. Jpn. **56**, 2259 (1987).
[29] T. F. Rosenbaum, K. Andres, G. A. Thomas, and R. N. Bhatt, Phys. Rev. Lett. **45**, 1723 (1980); T. F. Rosenbaum, R. F. Milligan, G. A. Thomas, R. N. Bhatt, and W. N. Lin, Phys. Rev. B **27**, 7509 (1983).
[30] T. G. Castner, Phys. Rev. Lett. **87**, 129701 (2001).
[31] R. N. Bhatt, Phys. Rev. B **26**, 1082 (1982).
[32] R. N. Bhatt, S. Bogdanovich, and M. P. Sarachik, Phys. Rev. Lett. **87**, 129702 (2001).
[33] T. F. Rosenbaum, G. A. Thomas, and M. A. Paalanen, Phys. Rev. Lett. **72**, 2121 (1994).
[34] T. G. Castner, Phys. Rev. B **61**, 16596 (2000).
[35] A. L. Efros and B. I. Shklovskii, *Electronic Properties of Doped Semiconductors* (Springer-Verlag, Berlin, 1984), Chap. 9.
[36] T. G. Castner, Phys. Rev. Lett. **84**, 2905 (2000).
[37] M. Watanabe, Y. Ootuka, K. M. Itoh, and E. E. Haller, Phys. Rev. B **58**, 9851 (1998).
[38] S. Timoshenko, *Theory of Elastic Stability* (McGraw-Hill, New York, 1936), p. 178.
[39] T. F. Rosenbaum (private communication).
[40] G. D. Watkins and F. S. Ham, Phys. Rev. B **1**, 4071 (1970).
[41] H. S. Tan and T. G. Castner, Phys. Rev. B **23**, 3983 (1981).
[42] D. W. Koon and T. G. Castner, Phys. Rev. B **41**, 12054 (1990).
[43] T. Trappmann, C. Sürgers, and H. v. Löhneysen, Europhys. Lett. **36**, 177 (1997).